Министерство образования и науки Российской Федерации
Санкт-Петербургский политехнический университет Петра Великого
Институт прикладной математики и механики
Высшая школа теоретической механики

Работа допущена к защите

Директор высшей школы

___________ А. М. Кривцов

«___»_______________20__ г.

ВЫПУСКНАЯ КВАЛИФИКАЦИОННАЯ РАБОТА МАГИСТРА

«ЧИСЛЕННОЕ МОДЕЛИРОВАНИЕ СЕЙСМИЧЕСКИХ ВОЛН И ПОДАВЛЕНИЕ ИХ ВОЗДЕЙСТВИЯ ПРИ ПОМОЩИ СЕЙСМИЧЕСКИХ БАРЬЕРОВ»

по направлению 01.04.03 «Механика и математическое моделирование»
по образовательной программе 01.04.03_02 «Механика и математическое моделирование (международная образовательная программа)»

Выполнил
студент гр. 3640103/80201 ____________ У. Полат

Руководитель
Доцент, к.ф.-м.н. ____________ Е. А. Подольская

Консультант
Научный сотрудник СПбПУ, к.ф.-м.н. ____________ В. А. Братов

Консультант
по нормоконтролю ____________ Е. А. Хайбулова

Санкт-Петербург

2020

Peter the Great St.Petersburg Polytechnic University
Institute of Applied Mathematics and Mechanics
Higher School of Theoretical Mechanics

Work approved

Head of the Higher school

___________ A. M. Krivtsov

«___»_______________20__ г.

GRADUATE QUALIFICATION WORK

«NUMERICAL SIMULATION OF SEISMIC WAVES AND MITIGATING THE EFFECTS BY SEISMIC BARRIERS»

Subject 01.04.03 «Mechanics and Mathematical Modeling»
Educational program 01.04.03_02 «Mechanics and Mathematical Modeling (international educational program)»

Submitted by
Student of group No.3640103/80201 ____________ U. Polat

Scientific advisor
Associate Professor, PhD. ____________ E. A. Podolskaya

Work advisor
Scientific researcher of SPbPU, PhD. ____________ V. A. Bratov

Regulatory
advisor ____________ E. A. Khaibulova

Saint Petersburg

2020

ABSTRACT

42 pages, 25 figures, 3 tables, 0 appendices

KEYWORDS: 2D NUMERICAL SIMULATION OF RAYLEIGH WAVE PROPAGATION, FINITE ELEMENT MODELING, VERTICAL SEISMIC BARRIERS, PASSIVE VIBRATION ISOLATION

The aim of this work is to study various seismic barriers with different material properties and dimensions to determine the optimal vibration mitigation rate and the effective protection zone against the Rayleigh wave. In order to observe the effects of seismic barriers, numerical simulation was implemented by utilizing ABAQUS finite element analysis software. Explicit Dynamic Analysis solver was applied to simulate Rayleigh wave propagation along the elastic half-plane. Reduction in the vibration energy of the Rayleigh wave was expected by placing vertical seismic barriers in the ground (passive vibration isolation) in front of the building which was intended to be protected. Further, the results of the numerical simulation were analyzed to determine the optimal barrier properties that provide effective protective zones (the area in which surface waves were attenuated). Thereafter, the results were verified by analytical solution. Applying vertical seismic barriers with different material properties and dimensions, 5.5 meter-depth seismic barrier with composite material was found the as the most efficient barrier since it provided longest effective protection zone (28 meters) behind the barrier. Therefore, the vibration energy of the Rayleigh wave can be mitigated thanks to seismic barrier up to an extent (nearly 89 per cent) by using such systems. Thence, the applicability of these systems is proved by numerical simulation results.

CONTENTS

LIST OF FIGURES

LIST OF TABLES

CHAPTER 1. INTRODUCTION

This research focuses on vibration energy isolation by implementing vertical seismic barriers. The following section has glanced at the history of earthquake and seismology evaluation.

1.1. History of the Earthquake

For centuries, humanity has been facing natural disasters in which earthquake takes the prominent place due to its frequent occurrence and the damage caused to the surrounding environment.

Urbanization and latest technological developments led to the formation of new sources of vibration. Nowadays, ground vibration is generated through various ways: Due to activities in construction sites, movement of high speed trains, demolition of buildings and earthquakes. Considering its high vibration energy and destruction potential, earthquakes were considered the most harmful vibration generating source amongst others. Thus, several studies have been carried out for the last decades to minimize the disruption to the surroundings by S.V. Kuznetsov, R. Motamed, A. Zerwer et al. etc. [8, 18, 20]

In this respect, Agnew [1] studied the history of earthquakes from 1755 till 1995 and manifested several researches that had been conducted in this period. The first thoughts about the cause of the earthquake were the idea of ground shaking. Later on, wave propagation motion was proposed as the reason for this natural disaster. Elasticity and gas pressure expansion inside the earth crust were presumed to be the actuating force of this motion. It was imagined that this motion resembles the movement of a curled carpet.

Subsequently, in the 19th century, further investigations were conducted to find a “pattern” between previous and recent earthquakes and to ascertain the relevance between these earthquakes. Due to breakages on the surface caused by the earthquakes in the 19th century, researchers presumed the possible cause of the earthquake as a series of faulting ruptures.

In 1829, S.D. Poisson had described the wave motion in the elastic medium [2]. He described the wave motion as two different waves in terms of their speeds and directions (the faster wave propagated in the direction of wave propagation and the slower wave propagated in the direction perpendicular to the wave propagation). By using elastic wave propagation theory, the motion of light sought to be elucidated as a motion of transverse waves in elastic "luminiferous ether".

In due course, in 1856, the first instrument to automatically record some aspects of the shaking was invented by L. Palmieri [1]. This instrument turned out to be inapplicable since it was designed to seek small motions that occur underground, rather than to detect high vibrations of earthquakes.

In 1885, the elastic surface wave explanation was suggested by Rayleigh [3]. The behaviour of waves upon a free elastic surface and the mathematical expression of Rayleigh wave characteristics were explained. It was acknowledged in the 19th century that the Earth mostly consists of solid along with hot liquid and gases. Therefore, it was assumed that elastic waves are transmitted through the surface and the depth of soil. However, the characteristics of these elastic waves were not clearly distinguished in that time due to anisotropic and inhomogeneous features of the soil.

Thenceforth, in 1904, Earthquake motion was explained with three different waves namely P, S and L according to their arrival times and velocities, not to their type [4]. Afterwards, by A.E.H. Love, extensive research was conducted on elastic waves [5]. It was found out that as surface waves propagate on the layered surface of the Earth, the particles move transverse to the propagation of wave motion. Further, a mathematical model of the surface waves was constituted.

Eventually, considerable focus was put on the surface wave studies to detect them before their occurrence since they are the most harmful seismic waves to the environment. To take countermeasures and alert the public about the earthquake before its occurrence, seismographs were invented by using new approaches and by using the seismic data which has been collected through years.

1.2. Types of Seismic Waves

During a seismic activity, four main wave types can be observed by utilizing a seismograph: Body waves such as Longitudinal (P-wave) and Transversal (S-wave) or surface waves that are encountered commonly: Rayleigh and Love waves. The propagation direction and velocity of each wave differ from each other as shown in Figure 1.

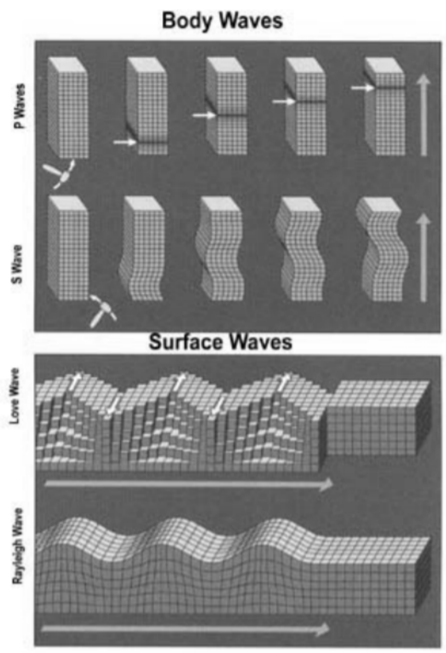

Figure 1. Propagation of the seismic waves [6]

The first wave that is spotted in the seismograph is the “Longitudinal wave” (Primary wave) due to it’s high velocity when it propagates in a medium. This wave can propagate in liquids, solids and gases unlike the other types of waves. As it propagates, the elements of the medium move with the push and pull movement (worm-like motion) and its speed can be calculated by equation (1). Since the propagation medium was considered as elastic, Lame constants were employed.

$$C_L = \sqrt{\frac{\lambda + 2\mu}{\rho}} \tag{1}$$

(λ and μ are Lame constants, ρ is material density (kg/m^3), C_L is the Longitudinal wave speed and C_T is the transversal wave speed)

After Longitudinal waves arrive, slower "Transversal waves" which have higher amplitude compared to Longitudinal waves can be observed. The propagation motion is transversal along the surface. Thence, while it is moving, particles move up and down perpendicular to the direction of propagation. The velocity of the Transversal wave C_T can be found as:

$$C_T = \sqrt{\frac{\mu}{\rho}} \tag{2}$$

In the seismograph, Rayleigh waves can be observed after Longitudinal and Transverse waves. The propagation motion is up and down along with the horizontal motion. The Rayleigh wave propagates on the surface and attenuates with increasing depth.

Since the Rayleigh wave travels along with the upper layer of the Earth crust, it contains localized, high vibration energy at the surface and the amplitude of vibration decreases with depth. Therefore, the effect of the Rayleigh wave will be the maximum on the surface where most of the constructions are built. The Rayleigh wave velocity C_R was estimated by Bergmann et al. in 1967 [7].

$$C_R = \frac{0.87 + 1.12\upsilon}{1 + \upsilon} C_T \tag{3}$$

1.3. Research Motivation

The idea to examine the related topic appeared due to the flaws of present-day vibration isolation systems in the sense of their vibration energy mitigation effectiveness. During a seismic activity, an effective vibration mitigating system should provide protection against repeated, low and high amplitude vibrations. At the same time, it should be economical to implement such a system.

Nowadays seismic protection systems are mostly built within the construction as an assembly (dampers) that moves separately from the building when an earthquake occurs. Another approach to mitigate the vibration energy is to plant a seismic barrier (horizontal or vertical) in front of the structure (as circulating the construction 360 degrees) to create a protection zone behind the barrier.

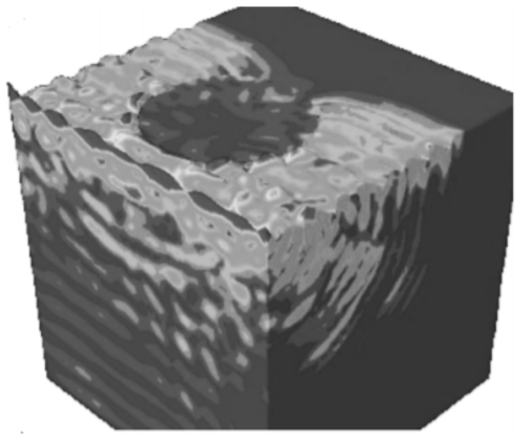

Figure 2. Vertical seismic barrier implementation as circulating the construction 360 degrees [8]

The limitations of the dampers that are built within the construction are high costs of setup and maintenance requirements. In addition, these systems have a definite lifetime that can bear the vibrations that are caused by the earthquakes. Thus, periodic maintenance and replacements of the parts whose lifetime finished are necessary.

Due to the stated reasons, usage of vertical or horizontal barriers seems advantageous since they don't require frequent maintenance and replacement, as well as the installation of such systems is inexpensive.

1.4. Research Objectives

The aim of this research is to study various vertical seismic barriers and to determine the optimal barrier properties for vibration energy mitigation. The main objectives of this study are presented below.

- Determining the effects of material properties of the barrier and barrier dimensions on the vibration energy reduction. Additionally, showing the effects of various wavelengths on the protection effectiveness.
- Constituting a 2D numerical model by using ABAQUS finite element modelling software.
- Indicating the effective protective zones that different vertical seismic barriers provide.
- Verifying the simulation results by comparing with the experimental data.

In order to simulate the effects of seismic barriers against the Rayleigh wave, numerical simulations were utilized by using ABAQUS finite element modelling software. Explicit Dynamic Analysis solver was implemented in the numerical simulation since the earthquake is a dynamical problem. By planting various seismic barriers with different material properties and dimensions in front of the structure which is aimed to be protected (placing the barriers around the building 360 degrees), the mitigation of the vibration energy was expected. Due to the computational cost of 3D modelling, 2D numerical modelling was implemented. Further, the results of the numerical simulation were analyzed to determine the optimal seismic barrier properties that provided effective protection against the Rayleigh wave. Following, the numerical simulation was validated by comparing with the data from the experiment from [11].

1.5. Thesis Outline

This thesis includes 8 chapters and references: Introduction, literature review, parametric study, a mathematical description of the problem, numerical simulation, numerical simulation results and summary.

In the first chapter, a brief overview of the history of Earthquake and the seismology development over the years was given. Following, the main types of seismic waves that are seen during the Earthquake are indicated. A motive for conducting this research was clarified in the Research Motivation section. As well, the objectives that needed to be achieved were presented.

In the second chapter, various researches that investigated Rayleigh wave propagation on elastic half-space are introduced. Characteristics of Rayleigh waves and methods of vibration isolation are presented in the Literature review.

In the third chapter, numerical simulation parameters are depicted and the results are presented. The parameters for the numerical simulation were chosen according to the parametric study.

In the fourth chapter, a mathematical description of Rayleigh wave motion on the elastic half-space is given. Along with that, the model was compared with the experimental results for validation purpose.

In the fifth and sixth chapters, a 2D model is created in ABAQUS and it is solved by implementing an explicit dynamic analysis method. Findings of the numerical solution are given.

In the last chapter, the summary of the results of this study are given.

CHAPTER 2. LITERATURE REVIEW

Many researchers focused on finding a solution for a wave propagation problem in a boundless medium based on the equations of Green and Stokes [9]. The characteristics of surface waves on the free surface were first described by Lord Rayleigh. He described the seismic event (which was produced by a single impulse) with two separate wave motions: “minor tremor” and “main shock”. Minor tremor occurs initially and may appear anywhere on the surface, at the same time subsides steadily causing the second motion. The second motion is called the “mainshock”. As this motion's propagation continues, its amplitude attenuates with the distance from the source.

The equations of motion in isotropic elastic medium were depicted as:

$$\rho \frac{\partial^2 u}{\partial t^2} = (\lambda + \mu)\frac{\partial \Delta}{\partial x} + \mu \nabla^2 u \qquad \text{(x-direction)} \tag{4}$$

$$\rho \frac{\partial^2 v}{\partial t^2} = (\lambda + \mu)\frac{\partial \Delta}{\partial y} + \mu \nabla^2 v \qquad \text{(y-direction)} \tag{5}$$

where λ and μ are Lame constants, ρ is material density. Displacement vectors in x and y directions were shown as u and v, while ϕ and ψ were scalar and vector potentials, Δ shows the gradient of displacement.

$$u = \frac{\partial \phi}{\partial x} + \frac{\partial \psi}{\partial y} \tag{6}$$

$$v = \frac{\partial \phi}{\partial y} - \frac{\partial \psi}{\partial x} \tag{7}$$

$$\Delta = \frac{\partial u}{\partial x} + \frac{\partial v}{\partial y}. \tag{8}$$

The attenuation of the Rayleigh wave on a free surface is described with equation (9).

$$\frac{1}{\sqrt{xr}} \tag{9}$$

where r is the number of waves and x is the distance from the epicenter. While body waves attenuate according to equation (10)

$$\frac{1}{|xr|} \tag{10}$$

This revealed that, as compared to body waves, Rayleigh waves attenuate with a much faster rate (exponentially) with distance.

In order to attenuate the Rayleigh waves, amplifying the roughness of the surface on the half-plane was considered by Goldstein et al. [10]. The author scrutinized the Rayleigh wave vectors and their interaction with rough surfaces. As these vectors are frequency-dependent (dispersive), the dispersion relations were used to explain the displacement field. Increasing the roughness of the surface caused the elastic medium to transform into a viscoelastic one. The maximum effect of surface roughness in the sense of wave attenuation was observed when small wavelengths were considered for the simulation.

An extensive research about vibration isolation systems was conducted by S.V. Kuznetsov [8]. In this research, recent studies, as well as the main ideas about the vibration protection implementations against surface waves were illustrated. In this regard, vertical and horizontal seismic barriers were examined. Implementation of an empty trench for the sake of attenuation of the Rayleigh wave was stated as impractical. As cited by Kuznetsov [8] "*For bulk waves the most effective vertical barrier would be an empty trench, or a trench filled in with a lighter material than the ambient soil.[...] However, propagating Rayleigh or Love waves will simply overflow an empty trench.*" Moreover, Love, Lamb, SH, Stoneley waves and their characteristics were pointed out. Lamb waves show similarities to the Rayleigh wave if the plane on which they propagate is isotropic and they are dispersive. Hence they can propagate on any material, including multiple anisotropic layered mediums. Contrary to Rayleigh waves, Stoneley waves are able to propagate on half-plane in a condition that material constants of the half-plane meet certain circumstances. Love waves propagate on the interface between elastic half-plane and the contacting layer as long as the following condition is satisfied: The bulk wave velocities of the elastic layer are greater than of the bulk waves in half-space.

$$C_{Halfplane} > C_{contact\,layer} \tag{11}$$

where C* represents speed of transverse waves.

SH waves show similarities to Love waves in terms of polarization. However, the existence of SH waves depends on the boundary condition. Along with the articulated waves above, their combination can also be observed such as Rayleigh-Lamb waves or Love-SH waves, if the propagation medium is multi-layered.

Another comprehensive investigation of vertical seismic barriers was performed by A. Alzawi et al. [11]. The effects of an open trench and seismic barriers with GeoFoam material against vibration isolation method were investigated. Seismic barrier dimensions and barrier location from the origin of vibration source and the effects of different load frequencies were inspected. Numerical simulation results were verified by the author with experiments which were conducted on the test site. Active (implementing the seismic barrier very close to the vibration generation source) and passive vibration screening methods (planting the seismic barriers very close to the structure which is aimed to be protected) were discussed. The amplitude reduction rate was calculated by dividing the maximum spectral velocity amplitude after implementation of a seismic barrier to the maximum spectral velocity amplitude before the implementation of the seismic barrier. Variations in the amplitude of reduction (in and out of phases) were associated with the phenomena of minima and maxima phenomenon. This phenomenon was firstly discovered by Woods [12] who carried out similar experimental procedure hitherto. After the experiment in the field, 2D simulation by finite element modelling was carried out with ABAQUS software to compare the simulation and experimental results. Implementation of open barrier provided average system effectiveness of 76 % and 89 % by numerical modelling and by field experiments respectively. By applying Eps Geofoam as a seismic barrier material, average system effectiveness was obtained of 64 % and 41 % by numerical simulation and by field experiment accordingly.

The small divergence was observed between the results of the experiment and the numerical simulation. Barriers that are deeper than 0.6 normalized distances (0.6λ), provided more effective protection compared to smaller barriers. Comparing with the field experiment, it is proved that 2D simulation utilizing the finite element method can provide realistic results.

In the study which was conducted by B. Qiu [13], seismic wave implementations near tunnels against the explosions were investigated. Blasting is often used in civil engineering since it is an economical way to remove material from the excavation site when it is encountered with the hard rocks foundation. As a result of these explosions, surface waves are generated. Hence it can be harmful to the surroundings as causing stress-induced damages. 2D finite element model was chosen for the simulation after a comparative study between 2D and 3D models. It was observed that the 2D model can provide adequately precise results and the simulation time is less expensive compared to the 3D model. Effects of the depth of the barrier, density and Young's modulus against the Rayleigh wave were investigated. By utilizing Python, the optimization of seismic barrier's properties was performed. As an outcome of this study, increasing the barrier density or reducing the Young's modulus can be effective to mitigate the vibration energy. At the same time, the Poisson ratio and damping ratio didn't exhibit any significant effect on the vibration reduction ratio. For this study soil deformation properties were not considered. Due to the complexity of the barrier geometry, proposals of seismic barrier designs were impractical.

In the review by M. E. Rahman et. al. [14], the methods for reducing the vibration energy was examined. The main focus was put on methods for protection against vibrations caused by transport systems such as high-speed trains, underground railways, etc. Vibrations on the surface can boost depending on the surface irregularities and inhomogeneity of the soil. As a method for vibration isolation, floating slabs were described. These systems are mainly used to reduce the vibration that is caused by high-speed trains. This system works well when the vibration frequency is less or equal to the resonant frequency. The effectiveness of such a system therefore depends largely on its design. Another method to diminish the vibration energy was introduced as a wave impending block. This system is generally implemented below the vibration inducing source and the effectiveness of this system depends on the stiffness of the impending block. As a third method, trenches were introduced for vibration energy isolation purpose. Active and passive screening methods were explained. The difference between these two methods solely depends on the location of the barrier. The aim of the active screening system is to attenuate the vibrations generated by the vibration source. This method is used to diminish the vibrations usually caused by high-speed trains. For a second approach, passive screening method is explained. It is used to protect the intended structure by placing the trench between the vibration source and the structure.

Train-induced wave propagation in layered soils using finite/infinite elements was studied by Yang et al. [15]. In the simulation model finite/infinite elements were used to avoid reflections at the boundaries, which could disturb the numerical simulation results. Cited by the Author [15], "*Using this method, both the material and geometric irregularities of soils in the near field and radiation damping in the far field can be easily taken into account*". The equation of motion in the frequency domain was described by equation (12).

$$([K]-\omega^2[M])\mathrm{s}=\mathrm{d} \tag{12}$$

where [K] is the stiffness and [M] is the mass matrices of the system. **s** and **d** were denoted as displacement and loading vectors respectively.

The attenuation of the vibration in ground was shown in equation (13).

$$L(dB)=20\log\frac{P_1}{P_2} \tag{13}$$

in which L is the attenuation in decibels, P_1 is the calculated attenuation and P_2 is a reference value.

In the homogeneous half-space the effects of the transverse wave velocity and the damping ratio on the velocities of the soil particles were investigated. Since there is a relationship between the speed of movement of the load and the speed of the transverse wave by the equation (14), decreasing the shear wave speed increased the Mach number (M) for the fixed value of the load movement speed (c). Therefore, higher vibration value in the field was observed by reducing the transverse wave velocity for a fixed value of the load movement velocity.

$$M = \frac{c}{C_T} \tag{14}$$

where M is the Mach number, c is the load moving speed and C_T is the transversal wave speed.

A change in the damping ratio had no effect on the velocity of the ground particles at subcritical speed of the moving load (c=70 m/s). At the supercritical speed of the moving load (c=100 m/s), however, the increase of the damping ratio led to a considerable reduction of the vibration energy.

Meta-barriers were used as a vibration isolation method by S. H. Kim and M. P. Das [16]. The authors used barriers which are composed of metamaterials to attenuate the seismic waves. The metamaterials are artificial homogeneous materials that are created in laboratory conditions to ensure smaller dimensions compared to wavelengths of the seismic waves. Using a passive screening method, the meta-barriers were placed between the vibration source and the structure to be protected. The implementation of the meta-barriers around the building created a shadow zone (protected zone behind the barrier where the amplitude of the vibrational energy is significantly reduced). As explained by the author [16] "*Metamaterials act as an attenuator by converting the seismic wave into an attenuated wave by making use of the imaginary velocity of the stop band of the wave. This method protects not only the building that is surrounded by metamaterials, but also all buildings behind the metamaterials*". A negative shear modulus was implemented by presenting Helmholtz resonator. Numerical simulation results of this study showed that the vibration energy of the seismic wave decreased as turning the seismic-wave vectors into the imaginary part of the equation. Most of the seismic wave energy were attenuated by transforming the vibration energy into sound and heat energy.

CHAPTER 3. PARAMETRIC STUDY

Finite element modelling of Rayleigh wave propagation was completed in accordance with the parametric study since the proper mesh size and the time increment are vital for the correct results.

The model parameters are chosen in reference to researches of A. Dudchenko [17] and A. Zerwer [18].

1. The size of the protected zone should not change which implies that the barrier volume can be replaced by its cross-section area as the barrier length remains constant.

2. To allow Rayleigh wave interaction, seismic barriers should satisfy the plane strain conditions. Therefore, the soil property of the model was designated according to plane strain condition.

3. The vertical model size H should satisfy the condition $H \geq \frac{C_L \tau}{2}$, where τ is the calculation time and C_L is longitudinal wave speed. The distance from the left border to the barrier should be $L_1 \geq \frac{C_L \tau}{3}$ while the observation zone is $L_2 = 2\lambda_{Rayleigh}$. The distance from the observation zone to the right border is $L_3 = \frac{C_L \tau - L_1 - L_2}{2}$. Hence, the total horizontal length L ought to be $L_1 + L_2 + L_3$. Considering the conditions above, the horizontal and vertical length was chosen to 110 x 75 meters.

4. The mesh element size should be smaller or equal to the lumped mass ς multiplied with the minimum wavelength $\lambda_{\min}$ [17].

$$g \leq \varsigma \lambda_{\min} \tag{15}$$

where constant ς is changing depending on the mass matrices being consistent (ς=0.25) or lumped (ς=0.2). Since the mass matrices were consistent in the numerical simulation, the value for this constant was taken as 0.25. Since the wavelength was selected as (2.98 m), the element size was chosen 0.3 meters.

5. The time increment τ should be less or equal to the element size g over the longitudinal wave velocity C_L.

$$\tau \leq \frac{g}{C_L} \tag{16}$$

For g = 0.3 meters and longitudinal wave speed being found from equation (16) C_L = 180.32 m/s, the time increment was chosen as 0.001 s.

6. During earthquakes, the maximum shear strains for the Rayleigh wave usually don't exceed $2x10^{-3}$ [19].

The maximum amplitude is taken as $2x10^{-3}$ meanwhile the frequency of harmonic excitation was chosen as 30 Hz by selecting the Rayleigh wavelength as 2.98 meters. To observe the effects of various wavelengths on the protection effectiveness, a harmonic load of 10 Hz, 15 Hz, 20 Hz and 30 Hz was applied to the model and the displacement rates were obtained with respect to distance from the barrier.

7. Vertical barriers should satisfy the following conditions in order to protect the given area from seismic waves effectively:

(i) The height of the barrier should be comparable with the lengths of the waves which it protects from. As following this principle, the depth of the seismic barriers was chosen bigger than the wavelength of the Rayleigh wave.

(ii) The material of the barrier should have higher Young's modulus and density than the ambient soil [8].

(iii) The shear modulus of the soil increases with the depth, as referring to the research of Motamed et al [20] (table 1).

Table 1. Young's modulus of soil in depth (from [20])

Depth (m)	**Young's Modulus (Pa)**
8.75	$5e^7$
17.5	$8e^7$

26.25	$11e^7$
35	$14e^7$

8. The material properties of the soil and the seismic barriers are listed in table 2. Soil is considered as dense sand.

Table 2. Material properties of seismic barrier materials [21]

Material	**Density ρ (kg/m³)**	**Young's Modulus E (Pa)**	**Poisson Ratio υ**	**Damping Ratio (%)**
Dense Sand	2070	5e7	0.3	0.01
Concrete 20/25	2400	$39e^9$	0.15	0.05
EPS GeoFoam	15	$28e^5$	0.09	0.05
Composite	1274.2	$97.5e^8$	0.12	0.05

9. In order to see the effectiveness of seismic barriers, a reduction factor $K_{reduction}$ was calculated by considering the following equation. [20]

$$K_{reduction} = \frac{A_{without} - A_{withbarrier}}{A_{without}} * 100 \qquad (17)$$

where $A_{without}$ represents the maximum acceleration amplitude before and $A_{withbarrier}$ stands for the maximum acceleration amplitude after placing a seismic barrier or empty trench.

10. The protection percentage was calculated according to the equation (18) to see the effects of different wavelengths on the protection percentage.

$$P = \frac{u_{plane} - u_{barrier}}{u_{plane}} * 100 \qquad (18)$$

In which $u_{barrier}$ represents the displacement field after implementation of the barrier, whilst u_{plane} is the displacement field of the half-plane before the implementation of the seismic barrier.

CHAPTER 4: MATHEMATICAL DESCRIPTION OF THE PROBLEM

Considering half plane for $-\infty < x \leq \infty$ and $y \geq 0$ with x and y being the coordinates of the elastic half-plane. The problem can be considered as a 2D plane strain problem since the plane elongates in z-direction infinitely.

The equation of motion in isotropic, elastic, homogenous media can be written applying the Navier-Clapeyron theorem [22]:

$$(\lambda + 2\mu)\nabla(\nabla.u) - \mu\nabla\times(\nabla\times u) + f\rho = \rho\frac{\partial^2 u}{\partial t^2} \tag{19}$$

Following, u can be expressed as applying Helmholtz decomposition theorem [23].

$$u = \phi \times \nabla s \tag{20}$$

Displacement vector u can be expressed in coordinates x and y by equation (21) and (22).

$$u_x = \frac{\partial\phi}{\partial x} - \frac{\partial s}{\partial y} \tag{21}$$

$$u_y = \frac{\partial s}{\partial x} + \frac{\partial\phi}{\partial y} \tag{22}$$

where ϕ and k are scalar and vector wave potentials for longitudinal and transversal waves and can be found by equations (23) and (24).

$$\phi = \Phi(y)e^{i(kx-\omega t)} \tag{23}$$

$$s = S(y)e^{i(kx-\omega t)} \tag{24}$$

where k is wave number, ω is the angular velocity. The unknown functions Φ(y) and S(y) can be written as below:

$$\Phi(y) = D_1\sin(py) + D_2\cos(py) \tag{25}$$

$$S(y) = L_1\sin(qy) + L_2\cos(qy) \tag{26}$$

in which the constants p and q can be written by equation (27) and (28).

$$p = \sqrt{w^2 / C_L{}^2 - k^2} \tag{27}$$

$$q = \sqrt{w^2 / C_T{}^2 - k^2} \tag{28}$$

Furthermore, governing equations for longitudinal and transversal waves can be written in equations (29) and (30) [24].

$$\frac{\partial^2 \Phi}{\partial x^2} + \frac{\partial^2 \Phi}{\partial y^2} = \frac{1}{C_L{}^2} \frac{\partial^2 \Phi}{\partial t^2} \quad \text{(for longitudinal waves)} \tag{29}$$

$$\frac{\partial^2 S}{\partial y^2} + \frac{\partial^2 S}{\partial y^2} = \frac{1}{C_T{}^2} \frac{\partial^2 S}{\partial t^2} \quad \text{(for transversal waves)} \tag{30}$$

Since the medium is elastic, the longitudinal and transversal wave speed (C_L and C_T) can be expressed using Lame constants μ and λ.

$$C_L = \sqrt{(E / \rho)} = \sqrt{((\lambda + 2\mu) / \rho)} \tag{31}$$

$$C_T = \sqrt{(G / \rho)} = \sqrt{(\mu / \rho)} \tag{32}$$

in which ρ is the material density, E is Young's modulus, G is the shear modulus. The Lame constants μ and λ can be found as:

$$\mu = \frac{E}{2(1+\upsilon)} \quad \text{and} \quad \lambda = \frac{E\upsilon}{(1-2\upsilon)(1+\upsilon)} \tag{33}$$

where, E is Young's modulus and υ is poisson ratio.

Considering longitudinal and transversal waves, substituting equation (31) and (32) into equation (19), the equation of motion in a linear elastic medium as a function of time can be obtained:

$$C_L{}^2 \nabla(\nabla . u) - C_T{}^2 \nabla \times (\nabla \times u) + f = \frac{\partial^2 u}{\partial t^2} \tag{34}$$

4.1. Initial Condition

Since there are no initial stresses in the half plane and at the symmetric boundary, initial conditions were taken as stated below:

$$u(r,t)\,|_{t=0} = 0 \tag{35}$$

$$\partial_t u(r,t)\,|_{t=0} = 0 \tag{36}$$

4.2. Boundary Condition

On the boundary surface of a half plane Ω, (considering the elastic, homogeneous and isotropic media) it is assumed that there are no tractions. Therefore, equation (37) can be used as a boundary condition.

$$t_\chi \equiv (\lambda\, tr(\nabla u)I + \mu(\nabla u + \nabla u^t)).\chi = 0 \quad \text{where } \Omega.\chi = 0 \tag{37}$$

where χ is the unit normal to the boundary surface Ω.

To describe the Rayleigh wave propagation equation on the half plane, u can be rewritten as substituting equation (23) and (24) into equation (20).

$$u = (\Phi(y)e^{i(kx-wt)} \times \nabla(S(y)e^{i(kx-wt)}) \tag{38}$$

Substituting equation (36) into equation (35) gives Rayleigh wave propagation on the free surface of the half plane.

$$\begin{aligned} t_\chi &= (\lambda tr(\nabla(\Phi(y)e^{i(kx-wt)} \times \nabla(S(y)e^{i(kx-wt)}))I \\ &+ \mu(\nabla(\Phi(y)e^{i(kx-wt)} \times \nabla(S(y)e^{i(kx-wt)})) + \nabla(\Phi(y)e^{i(kx-wt)} \times \nabla(S(y)e^{i(kx-wt)})^t).\chi = 0 \end{aligned} \tag{39}$$

At the interface between soil and seismic barrier ideal mechanical contact was used.

$$\begin{aligned} t_{barrier} &= t_{soil}\,|_{\text{int}erface} \\ u_{barrier} &= u_{soil}\,|_{\text{int}erface} \end{aligned} \tag{40}$$

where $u_{barrier}$ and u_{soil} are displacement vectors on the contact surface of the soil and seismic barriers at the interface, $t_{barrier}$ and t_{soil} are surface stresses on the interface surface of the barrier and the soil.

CHAPTER 5. NUMERICAL SIMULATION

An elastic half-space (110 x 75m) consisting 35982, 4-node bilinear, plane strain quadrilateral elements of the element type “CPE4R” was implemented for the model. The left model border was taken as symmetric in order to reduce the calculation time. At the bottom and the right side of the plane, infinite elements of the element type “CINPE4” were utilized to avert reflections from the boundaries which can affect the solution. The chosen element types are illustrated in Figure 3.

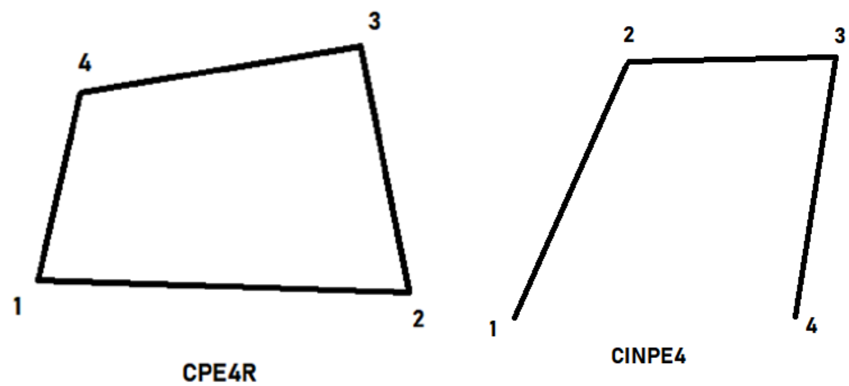

Figure 3. Chosen element types

A harmonic load was applied at the top left side where the symmetry condition was set. The harmonic excitation was given according to the function $A\sin(2\pi.f.t)$, where A is maximum amplitude, f is frequency and t is cumulative time.

In a distance of 32 m from the applied load (symmetry border), a 1.8 meters-width seismic barrier was placed. The dimensions of the barrier were chosen according to the parametric study to ensure optimal protection against Rayleigh wave propagation. Different depths for the barriers were considered as shown in Figure 6.

Three different material properties were chosen for the seismic barriers: EPS, concrete and the composite which consists of EPS and concrete. Along with these barriers, an open trench was considered for the simulation.

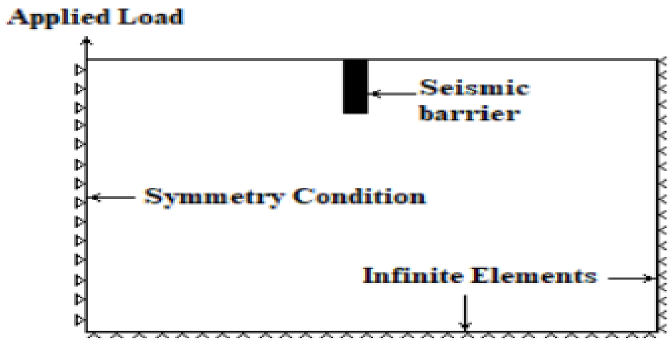

Figure 4. The model with infinite elements and boundary conditions

The numerical simulation was completed using an explicit finite difference method with ABAQUS 6.14-5.

The following explicit central difference formula was used for the iteration:

$$\dot{U}^{N}_{(\alpha+1/2)} = \dot{U}^{N}_{(\alpha-1/2)} + \frac{\Delta t_{(\alpha-1)} + \Delta t_{\alpha}}{2}\dot{U}^{N}_{(\alpha)} \tag{41}$$

where U^N is a degree of freedom, subscript “α” number of increments and Δt is the time increment [24].

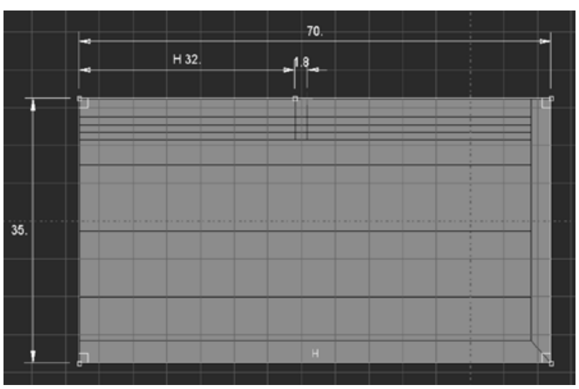

Figure 5. Elastic half space dimensions (m)

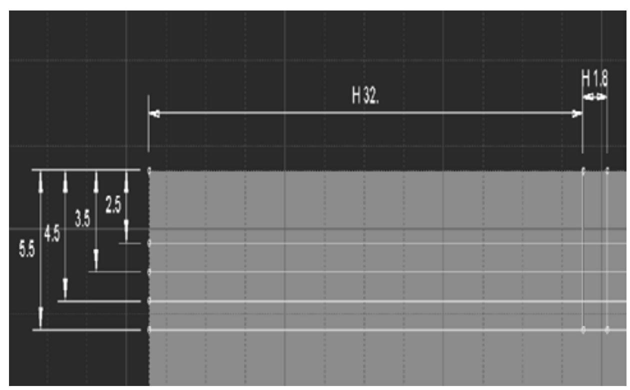

Figure 6. Various depths of the seismic barrier (m)

Several sensor points were selected to observe the Rayleigh wave vibration effects behind the barrier. The location of the sensor points are illustrated in Figure 7 and listed in Table 3.

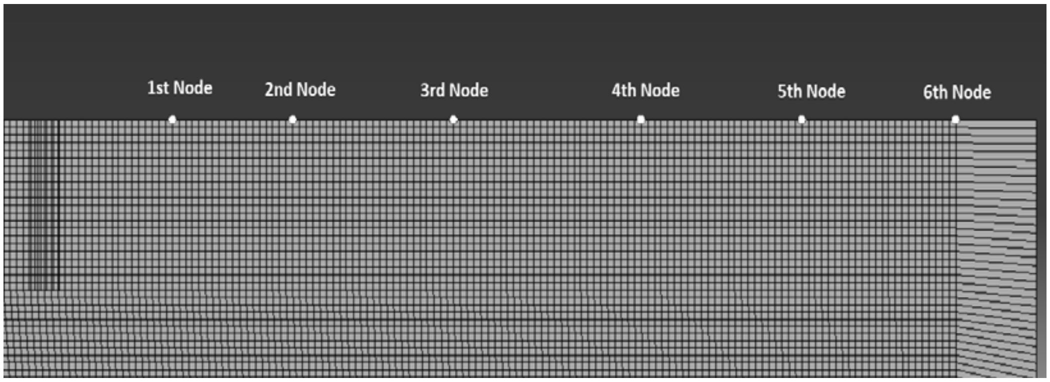

Figure 7. Location of the sensor points

Table 3. Locations of the sensor points

Sensor point number	1	2	3	4	5	6
Distance from seismic barrier (m)	5.2	10.7	15.4	22.2	28.2	33.2

CHAPTER 6. RESULTS OF THE NUMERICAL SIMULATION

6.1. Simulation Results for Open Trench

The maximum acceleration rates in distance from the barrier are shown for the different empty barrier depths compared to no barrier in figure 8.

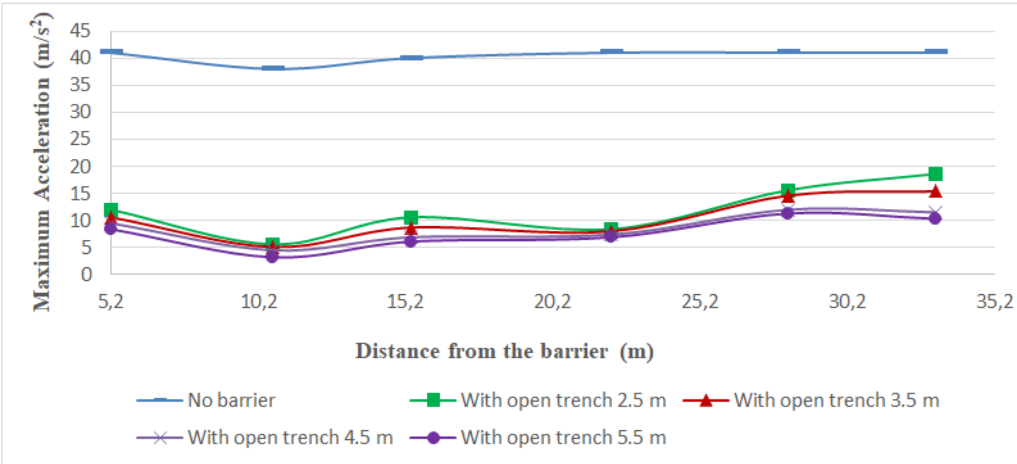

Figure 8. Maximum acceleration rates after implementing empty trench

Placing open trenches decreased the maximum acceleration amplitude up to around 4 m/s^2. It was observed that by increasing the depth of the trench, more reduction in the amplitude of the Rayleigh wave can be achieved.

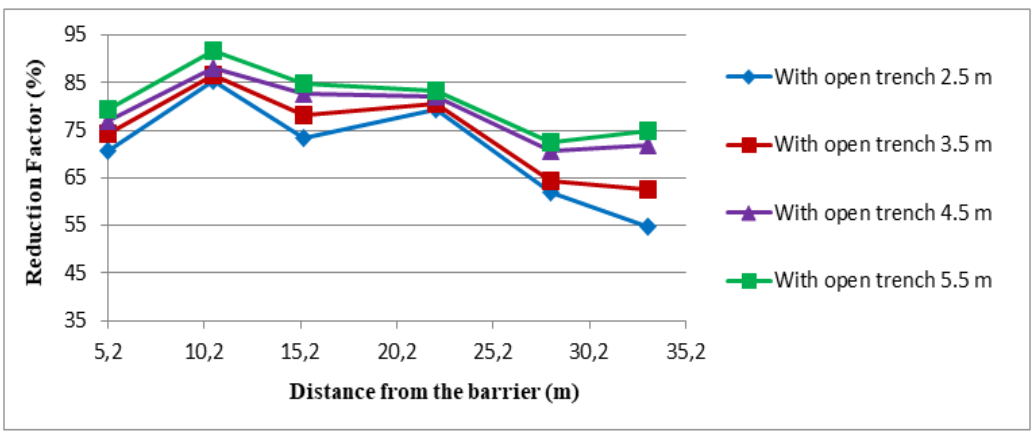

Figure 9. Reduction factors after implementing an empty trench

In figure 9, the reduction factor with distance from the barrier is visualized for different depths of the empty barrier. The reduction factor was obtained up to 91 per cent with a 5.5-meters depth empty trench. As it can be monitored from the graph, after 10 meters, the vibration energy steadily decreased. Thus, the statement of S. Kuznetsov [8] “*However, propagating Rayleigh or Love waves will simply overflow an empty trench*.” is confirmed. Rayleigh waves overflew the empty trench after 10 meters. Therefore, by implementing an empty trench, an effective protection zone of 10 meters can be reached.

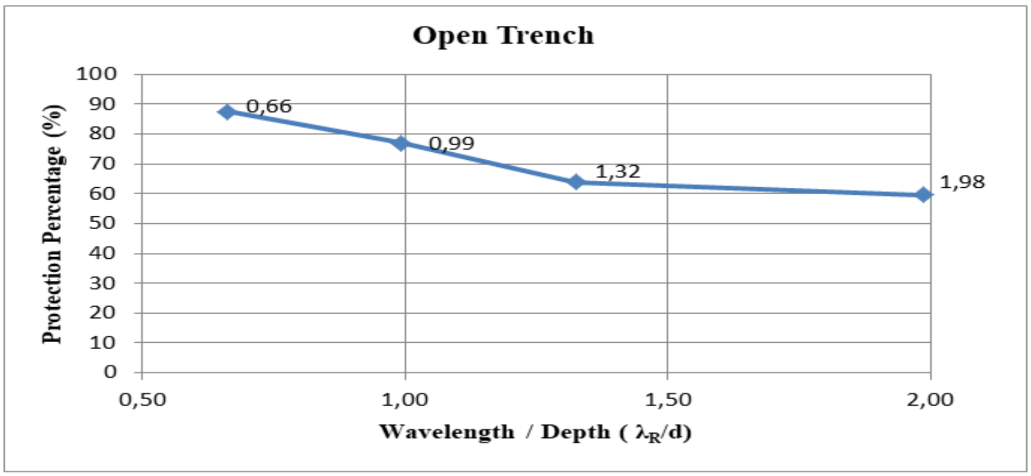

Figure 10. Protection percentages for open trenches with respect to the wavelength-depth ratio for fixed barrier depth (4.5 m)

For the fixed barrier depth (4.5 m), increasing the wavelength of the Rayleigh wave (decreasing the frequency of applied load) caused a reduction in the protection percentage around 30 % after the Rayleigh wavelength became longer than the fixed barrier depth.

6.2. Results for Seismic Barrier with Concrete 20/25

In a second step, the seismic barrier was built with concrete 20/25. The maximum acceleration with distance from the barrier is shown in Figure 11.

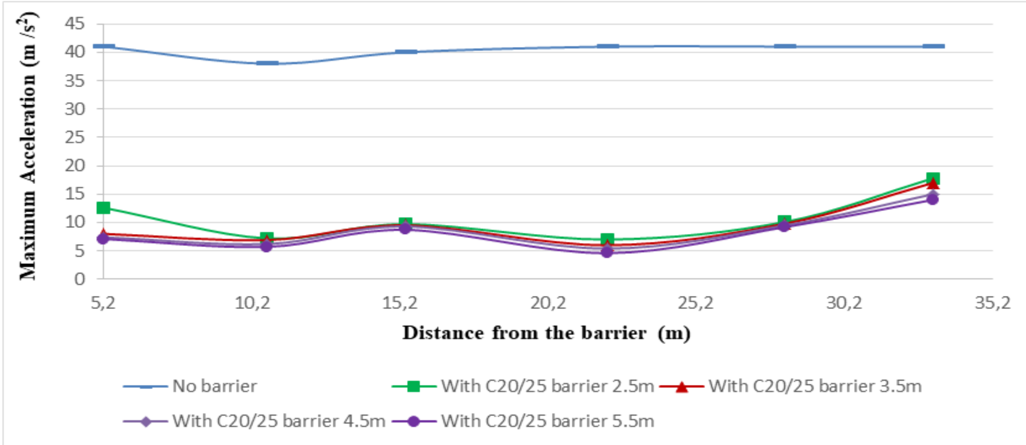

Figure 11. Maximum acceleration rates after placing barrier with Concrete 20/25

After planting a seismic barrier with Concrete 20/25, the maximum acceleration dwindled to 4.6 m/s. Additionally, it was observed that the maximum acceleration with Concrete 20/25 was around a ten per cent of the maximum acceleration without barrier.

It was observed in figure 11 that, after 22 meters, the maximum acceleration rate steadily increased.

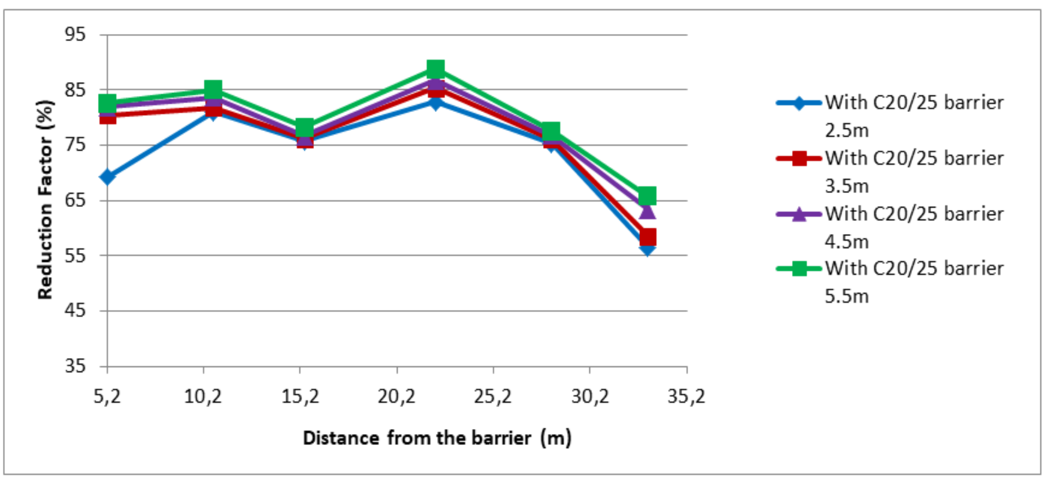

Figure 12. Reduction factors in the acceleration after placing seismic barrier with Concrete 20/25

Reduction factor in the acceleration was obtained as 88 per cent by using Concrete 20/25 material for the seismic barrier. As can be observed, after 22 meters away from the barrier, the acceleration reduced due to attenuation of the wave with distance. Increasing the depth of the barrier escalated the reduction factor. Thus, the effective protection zone was remarked as 22 meters.

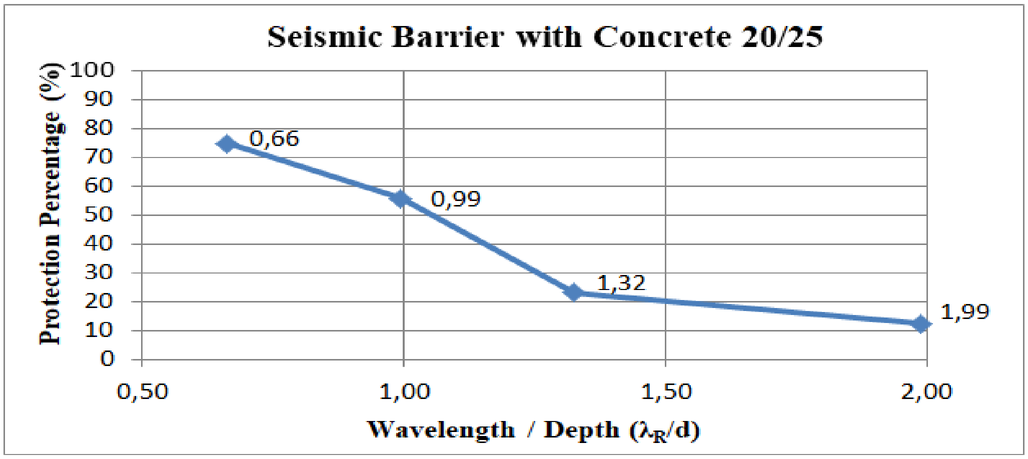

Figure 13. Protection percentages for a seismic barrier with Concrete 20/25 with respect to the wavelength-depth ratio for fixed barrier depth (4.5 m)

Increasing the wavelength reduced the protection factor greatly for the seismic barrier with Concrete 20/25. Therefore, to obtain effective protection with Concrete 20/25, the height of the barrier should be chosen higher than the Rayleigh wavelength.

6.3. Results for Seismic Barrier with Eps Geofoam

In the next step, the seismic barrier was built with Eps Geofoam. The maximum acceleration with distance from the barrier is shown in Figure 14.

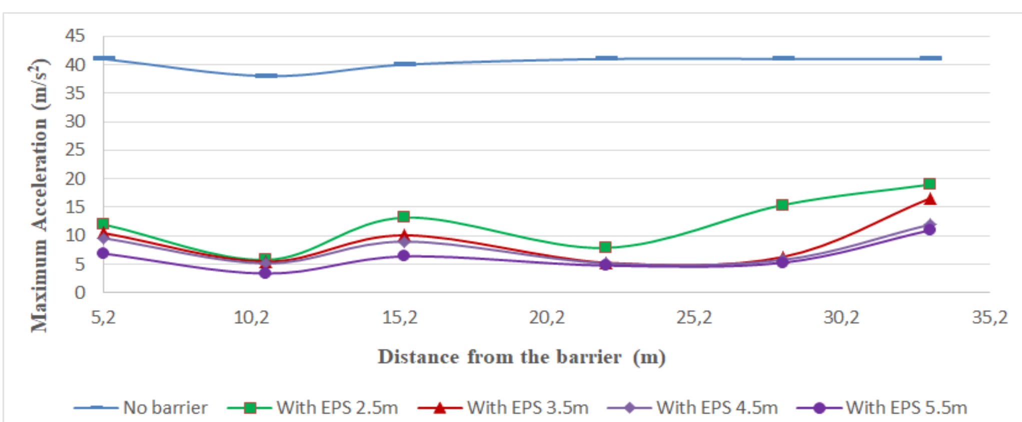

Figure 14. Maximum acceleration rates after placing barrier with Eps Geofoam

Applying Eps as a seismic barrier material lessened the maximum acceleration amplitude to 3.4 m/s^2 (figure 14). Placing the seismic barrier with a depth of 5.5 meters resulted in a maximum reduction in the acceleration.

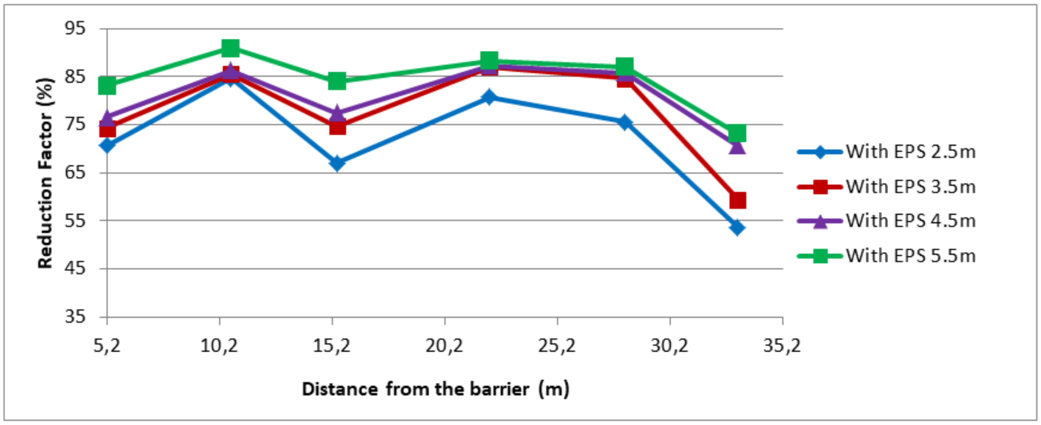

Figure 15. Reduction factors in the acceleration after placing seismic barrier with Eps Geofoam

As can be monitored from Figure 15, 91 % of the reduction in the displacement was gained by applying 5.5 meters-depth seismic barrier with Eps GeoFoam. The effective protection zone was attained at 28 meters.

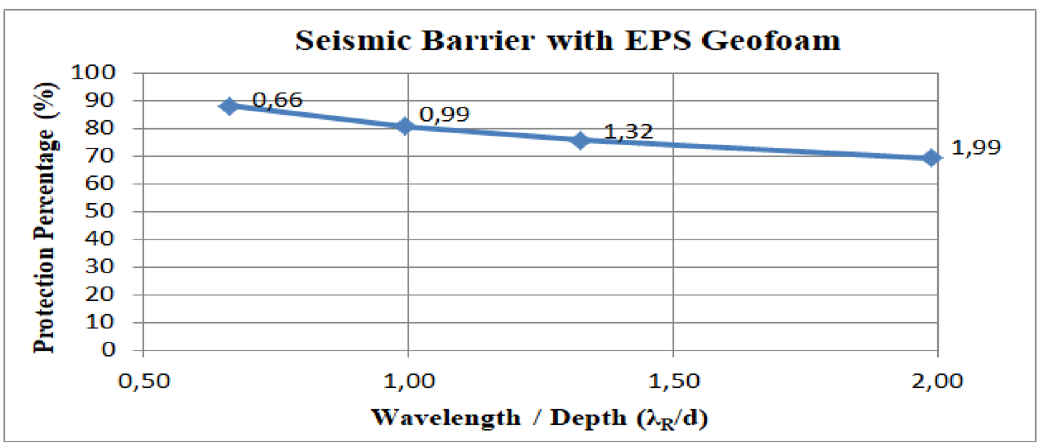

Figure 16. Protection percentages for a seismic barrier with Eps Geofoam with respect to the wavelength-depth ratio for fixed barrier depth (4.5 m)

Increasing the wavelength reduced the protection percentage (figure 16). For wavelengths bigger than the seismic barrier depth (4.5 meters), the protection percentage diminished below 80 %.

6.4. Results for Seismic Barrier with Composite Material

For the last simulation, a composite material which consists of Eps Geofoam and Concrete 20/25 was implemented to a seismic barrier. In figure 17, the maximum acceleration rates are shown.

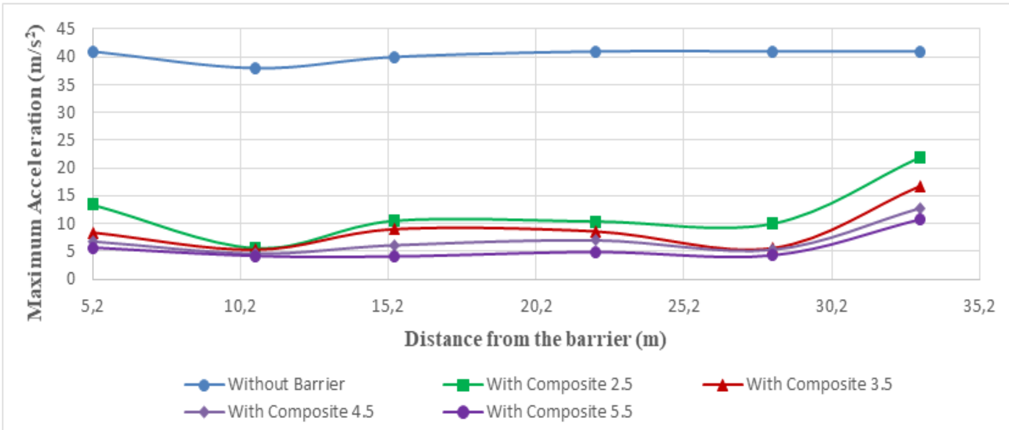

Figure 17. Maximum acceleration rates after placing barrier with Composite

Up to an acceleration of 5.2 m/s^2 was realized when a 5.5-meter depth barrier was planted. After 28 meters, a soar in the maximum acceleration was noticed.

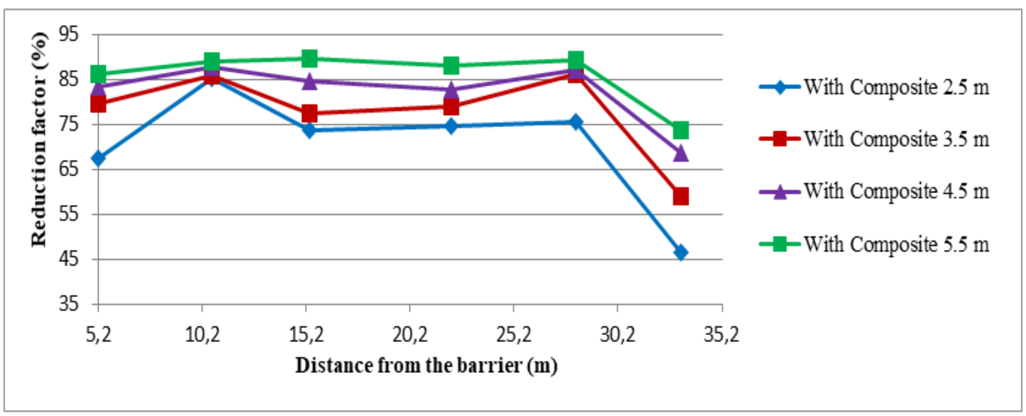

Figure 18. Reduction factors in the acceleration after placing seismic barrier with Composite material (Eps and Concrete 20/25)

Applying composite (Eps Geofoam and Concrete 20/25) helped the reduction factor to reach 89 per cent while increasing the depth contributed to a rise in the acceleration as can be seen in figure 18. Furthermore, composite material provided the longest effective protection zone (around 28 meters) among the other seismic barriers.

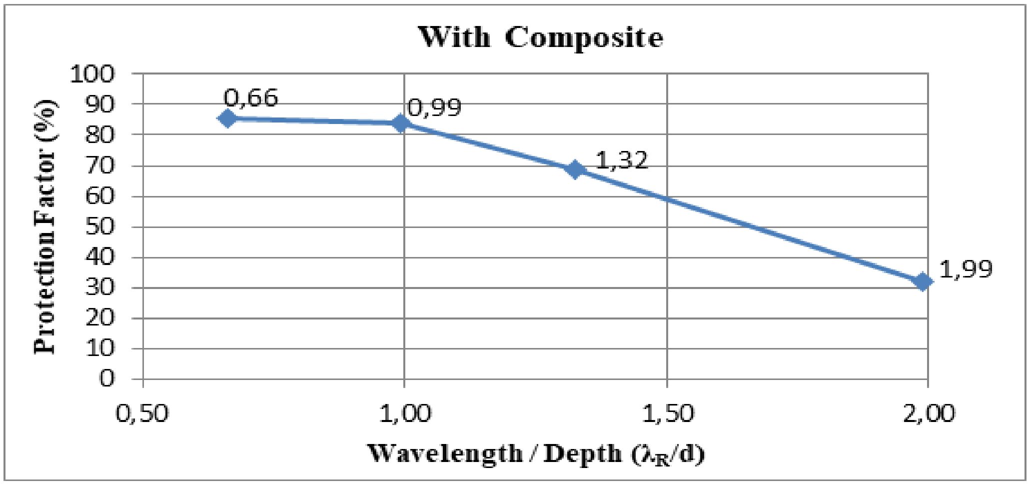

Figure 19. Protection percentages for a seismic barrier with Composite material with respect to the wavelength-depth ratio for fixed barrier depth (4.5 m)

As it was observed in figure 19, for wavelengths bigger than the barrier depth, the protection percentage linearly falls to 30 per cent. For the wavelengths higher than the seismic barrier depth, the protection percentage diminished visibly.

6.5. Validation of the Simulation Results

To validate the model of the numerical simulation, experimental findings of the study which was conducted by A. Alzawi et al. [11] were taken for comparison. The simulation was modelled with 2D plane strain conditions and solved numerically in ABAQUS by utilizing the explicit dynamic method. The same material properties, dimensions and constants as in the previous model were used to validate the presented numerical model. The load, boundary condition, dimensions and the location of the barrier were taken according to the experimental study to compare the results.

In the experimental study, an open trench and Eps GeoFoam barrier of 3 meters-depth, 0.25-width was utilized. As a load, a harmonic sinusoidal force of 23.5 kN was applied to the ground with the frequencies of 40 Hz, 50 Hz and 58.84 Hz.

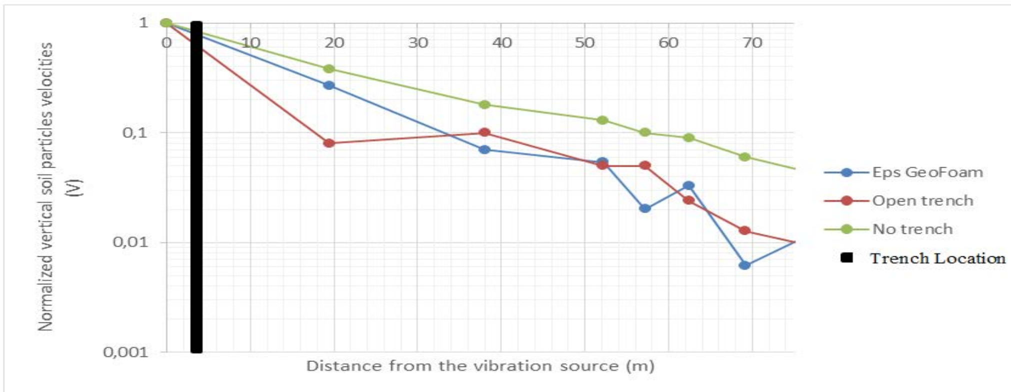

Figure 20. Numerical simulation results of replicating the experiment of vibration with 40 Hz

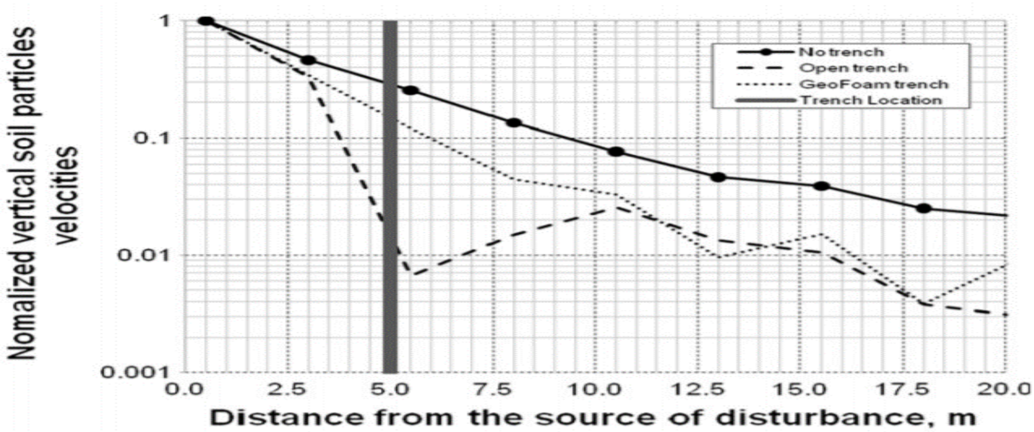

Figure 21. Experimental results of replicating the experiment with 40 Hz (from [11])

Comparing the figure 20 and figure 21, it can be observed that results of the numerical simulation and experimental results followed a similar pattern. Due to the reflections from the boundaries and the inhomogeneities in the soil, variations in the vertical soil particle velocities were observed. However, in both results, Eps Geofoam trench reduced the speed of soil particles to a minimum rate as a comparison to no trench and open trench graphs.

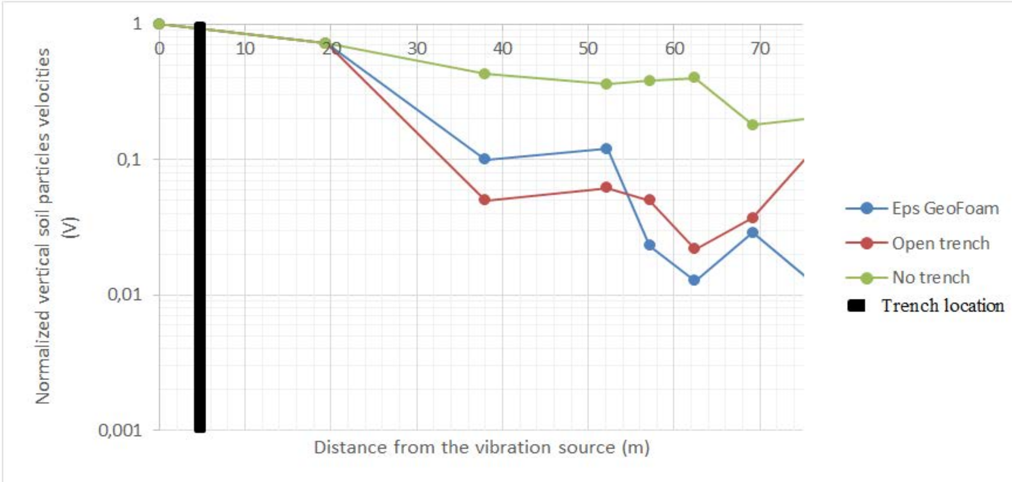

Figure 22. Numerical simulation results of replicating the experiment of vibration with 50 Hz

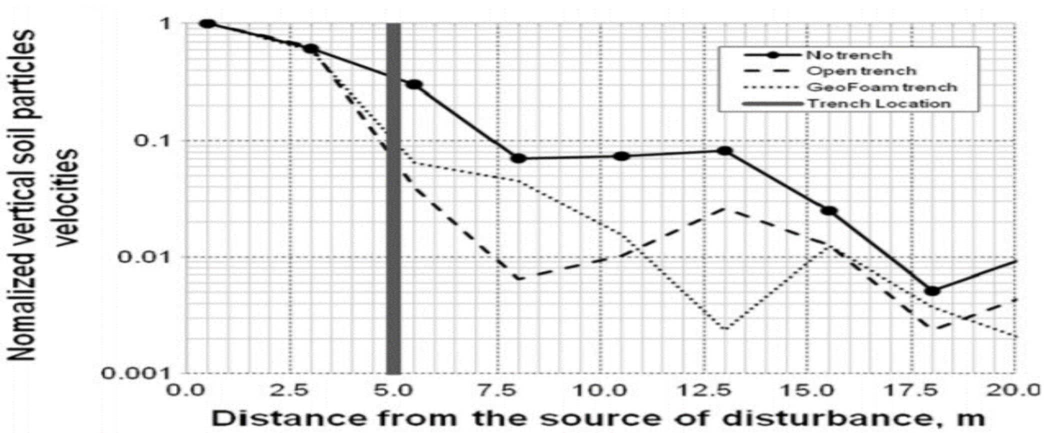

Figure 23. Experimental results of replicating the experiment with 50 Hz (from [11])

As the frequency increases, the effectiveness of open trench increases in the sense of vibration isolation. By applying 50 Hz frequency as a harmonic load, the normalized vertical soil particles velocities diminished compared to 40 Hz frequency load.

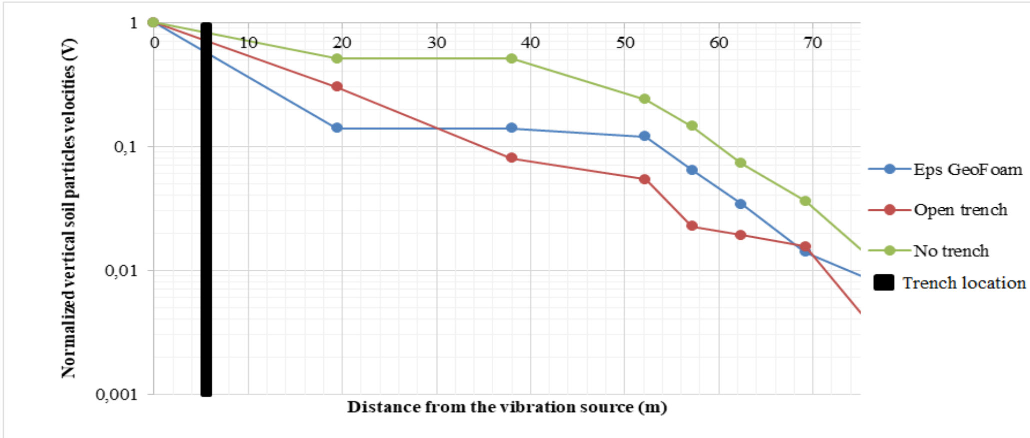

Figure 24. Numerical simulation result of replicating the experiment of vibration with 58.84 Hz

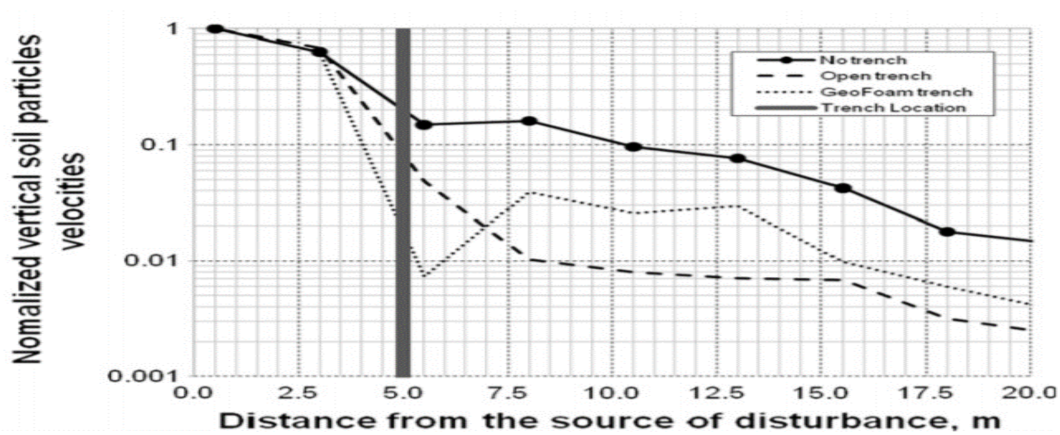

Figure 25. Experimental results of replicating the experiment with 58.84 Hz (from [11])

For the applied frequency of 58.84 Hz, a steady descent in the soil particles velocities was observed for the open and no trench. The open trench was spotted to be the most effective vibration isolation method for the applied load of 58.84 Hz.

Comparing the experiment and the simulation results, the model can be assumed as validated.

CHAPTER 7. SUMMARY

In summary, the following results can be mentioned:

- Increasing the barrier depth was proved to be helpful for the sake of vibration isolation for all the seismic barriers types.
- Stiffer material (Concrete 20/25) provided an acceleration reduction rate of 88 % and 22 meters of the protection zone. Therefore, applying concrete as a seismic barrier material can be helpful to get a reasonable reduction and protection zone.
- Empty trenches provided very effective but shallow protection as granting 10 meters of protection zone with 91 per cent acceleration reduction rate. The sudden decrease in the acceleration rate after 10 meters was associated with the Rayleigh wave overflowing the empty trench and continuing its propagation along the half-plane.
- EPS Geofoam rendered satisfactory reduction in the vibration energy (91 %). However, the obtained effective protection zone was similar to the protection zone when using the stiffer concrete material (22 meters).
- Applying composite material, which is composed of Geofoam and Concrete 20/25, was found out to be the most effective method since it provided the longest protection zone (28 meters) and at the same time 89 per cent acceleration reduction rate was achieved.
- Repeating the field experiment of A. Alzawi et al. [11] by numerical modelling manifested similar patterns of the velocity of soil particles graphs. Therefore, this constituted a validation for the numerical model.

All in all, this study considered Rayleigh wave propagation on the free surface of elastic, homogenous, isotropic half-plane. 2D numerical simulation was created utilizing ABAQUS. As a result, optimal barrier materials and dimensions were obtained. A seismic barrier with 5.5 meter-depth composite material which is composed of rigid Concrete 20/25 and softer Eps Geofoam was found out to be most effective seismic barrier.

REFERENCES

[1] Agnew, D. C., & Lee, W. H. K. (2002). History of seismology. International handbook of earthquake and engineering seismology, 81(A), 3-11.

[2] Poisson, S. D. (1835). Théorie mathematique de la chaleur mémoire et notes formant un supplement à l'ouvrage publié sous ce titre par SD Poisson. Bachelier.

[3] Rayleigh, L. (1885). On waves propagated along the plane surface of an elastic solid. Proceedings of the London mathematical Society, 1(1), 4-11.

[4] Wiechert, E. (1904). Verhandlungen der zweiten internationalen Seismologischen Konferenz. Gerlands Beitr. Geophys, 2, 41-43.

[5] Love, A. E. H. (1898). The scattering of electric waves by a dielectric sphere. Proceedings of the London Mathematical Society, 1(1), 308-321.

[6] The figure was taken from https://en.wikipedia.org/wiki/Seismic_wave at 28.05.2020

[7] I. A. Viktorov. Rayleigh and Lamb Waves: Physical Theory and Applications. Translation From Russian. With a Foreword by Warren P. Mason. Plenum press, 1967.

[8] Kuznetsov, S. V. (2011). Seismic waves and seismic barriers. Acoustical Physics, 57(3), 420-426.

[9] H. Lamb. On the propagation of tremors over the surface of an elastic solid. Proceedings of the Royal Society of London, 72(477-486):128: 130, 1904.

[10] Goldstein, R. V., & Lewandowski, J. (1992). Surface roughness induced attenuation and changes in the propagation velocity of long Rayleigh-type waves. Acta mechanica, 91(3-4), 235-243.

[11] Alzawi, A., & El Naggar, M. H. (2011). Full scale experimental study on vibration scattering using open and in-filled (GeoFoam) wave barriers. Soil Dynamics and Earthquake Engineering, 31(3), 306-317.

[12] Woods RD. Screening of surface waves in soil. Journal of Soil Mechanics and Foundation Engineering(ASCE)1968;94(SM4):951–79.

[13] Qiu, B. (2014). Numerical study on vibration isolation by wave barrier and protection of existing tunnel under explosions (Doctoral dissertation).

[14] Rahman, M. E., & Orr, T. (2006). A review of strategies to control manmade induced Ground vibrations. In Proceedings of The 13th International Congress on Sound and Vibration, Vienna.

[15] Yang, Y. B., Hung, H. H., & Chang, D. W. (2003). Train-induced wave propagation in layered soils using finite/infinite element simulation. Soil Dynamics and Earthquake Engineering, 23(4), 263-278.

[16] Kim, S. H., & Das, M. P. (2013). Artificial seismic shadow zone by acoustic metamaterials. Modern Physics Letters B, 27(20), 1350140.

[17] Dudchenko, A. (2018). Numerical analysis of surface Rayleigh wave interaction with seismic barriers and pile fields accounting elastic-plastic soil behaviour (Doctoral dissertation).

[18] Zerwer, A., Polak, M. A., & Santamarina, J. C. (2003). Rayleigh wave propagation for the detection of near surface discontinuities: Finite element modeling. Journal of nondestructive evaluation, 22(2), 39-52.

[19] J. F. Semblat and A. Pecker. Waves and vibrations in soils: earthquakes, traffic, shocks, construction works, 2009.

[20] Motamed, R., Itoh, K., Hirose, S., Takahashi, A., & Kusakabe, O. (2009). Evaluation of wave barriers on ground vibration reduction through numerical modeling in ABAQUS. In Proceedings of the SIMULIA Customer Conference 2009 (pp. 402-441).

[21] The material properties were taken from https://www.academia.edu/8149496/_APPC-Soil_Properties at 04.06.2020

[22] François, D., Pineau, A., & Zaoui, A. (1998). Mechanical behaviour of materials. Dordrecht: Kluwer academic publishers..

[23] Morino, L. (1986). Helmholtz decomposition revisited: vorticity generation and trailing edge condition. Computational Mechanics, 1(1), 65-90

[24] Wang, T. (2014). Finite element modelling and simulation of guided wave propagation in steel structural members